Detecting Anomalies in Measured Thermal Neutron Flux Profiles of SAFARI-1 Research Reactor

Rethabile Kgolobe[1], Pavel M. Bokov[3], Simon H. Connell[2], Charis Harley[1], Bongani G. Maqabuka[2,3], Lesego E. Moloko[3], and Rian H. Prinsloo[3]

[1]Electrical and Electronic Engineering Science, University of Johannesburg, Johannesburg, South Africa

[2] Mechanical Engineering Science, University of Johannesburg, Johannesburg, South Africa

[3] The South African Nuclear Energy Corporation (Necsa), Pretoria, South Africa

E-mail: rethabilethuto3@gmail.com

Abstract. Accurate measurement, analysis, and correct interpretation of the neutron flux distribution within the reactor core are essential for safety, performance, and operational information. In SAFARI-1, the axial thermal neutron flux profiles are measured at the beginning of each operational cycle using copper wires. This study investigates changes in these profiles caused by the control rod movement, focusing on key features of the flux profile: bottom minimum, peak maximum, and top minimum, to estimate anomalies. The approach involves data preprocessing, visualization, and statistical analysis. Polynomial fits were applied to smooth the data and extract key feature points, standard deviation, mean absolute deviation, Pearson's Correlation Coefficient, and other correlation metrics to assess flux profiles' sensitivity to control bank positions. A statistical method based on the likelihood of the data compared to specific models was also used to estimate errors and determine correlations. Results demonstrated that the top minimum points remained consistent and less correlated to bank positions, confirming its suitability for estimating anomalies. This approach improves the accuracy of detecting axial shifts from incorrect wire insertion and neutron flux measurements. Hypothesis testing at a 95% confidence level validates the trend behavior tracking control rod bank positions.

1 Introduction

In nuclear reactors, such as the SAFARI-1 (South African Fundamental Atomic Research Installation-1) research reactor, accurate measurements of neutron flux distributions are crucial as they contribute to monitoring the reactor core parameters, ensuring safety, and optimum performance during reactor operations [1]. The SAFARI-1 reactor is a 20 MW pool-type Material Testing Reactor (MTR), located at Pelindaba, South Africa, and is operated by the South African Nuclear Energy Corporation SOC Ltd (Necsa). It is designed in an 8×9 core grid structure that accommodates 26 fuel, 6 follower-type control rod assemblies, and other components, which are explained in detail in [2]. The SAFARI-1 core top view, fuel and control assemblies top view with fuel plates and the copper wire insertions in the assemblies are shown in Figure 1.

In SAFARI-1, axial neutron flux profiles are measured at the beginning of each operational cycle [3]. The measurements are conducted by inserting natural copper wires along the length of each of the 32 assemblies, containing fissile material, of which 26 are fuel and 6 are control assemblies. The radioactive β decay of the ^{64}Cu with a half-life of 12.7 h, is measured at 180 points along the wire for the 32 assemblies and stored in the datasets [4]. The resulting data are used to analyze the distribution of neutron flux and power, estimate core parameters such as peak-clad temperatures, and support detection of anomalies such as fuel element missloads [1]. However, the

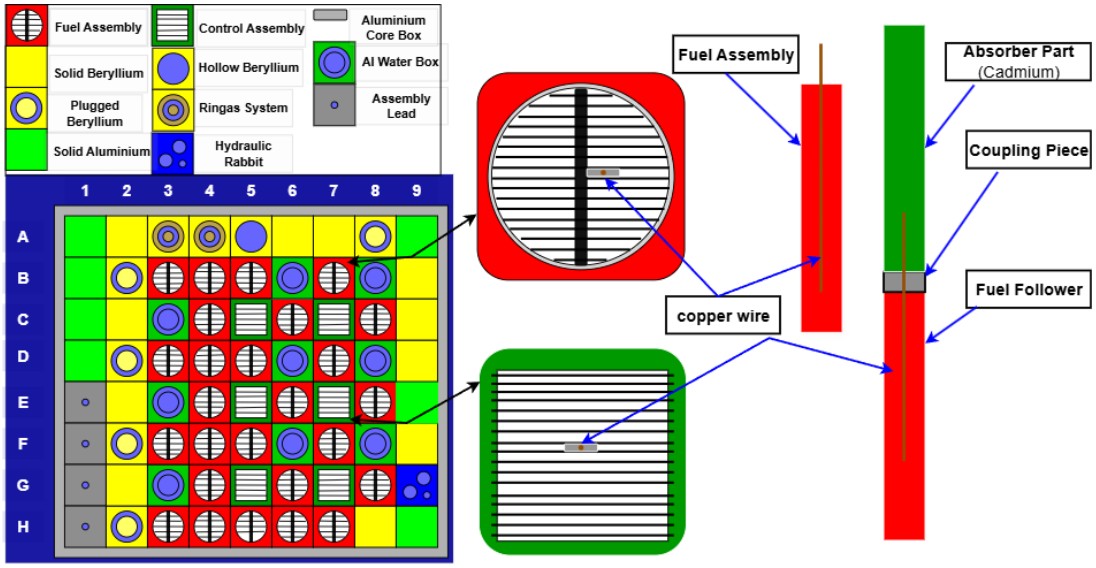

Figure 1: The SAFARI-1 core top view and fuel and control assemblies with fuel plates (left and middle) and side view (right).

accuracy and reliability of these measured neutron flux distributions depend on the accuracy of the copper wire measurement process, such as the correct insertion of the copper wire in the assemblies.

The manual insertion of the wires may result in inaccurate measurements, such as an axial shift in neutron flux, which can potentially lead to misinterpretations and wrong operational decisions. Note that in these experiments, relative activity shapes across the core are of primary concern (reactor power is quite uncertain at the low power levels during the experiment). Although techniques exist to analyze and detect axially shifted measurements of the neutron flux, mathematically-backed methods for detecting anomalies due to copper wire incorrect insertions in the SAFARI-1 research reactor would be of great value. In this study, statistical techniques are used to detect anomalies in the neutron flux measurements caused by the incorrect insertion of copper wires, focusing only on fuel assemblies. By analyzing the key features of the neutron flux profiles specifically, the bottom minimum, maximum, and top minimum (as indicated in Figure 2), the research aims to develop techniques that will detect anomalies in the neutron flux profiles caused by incorrect copper insertion in the SAFARI-1 research reactor. The

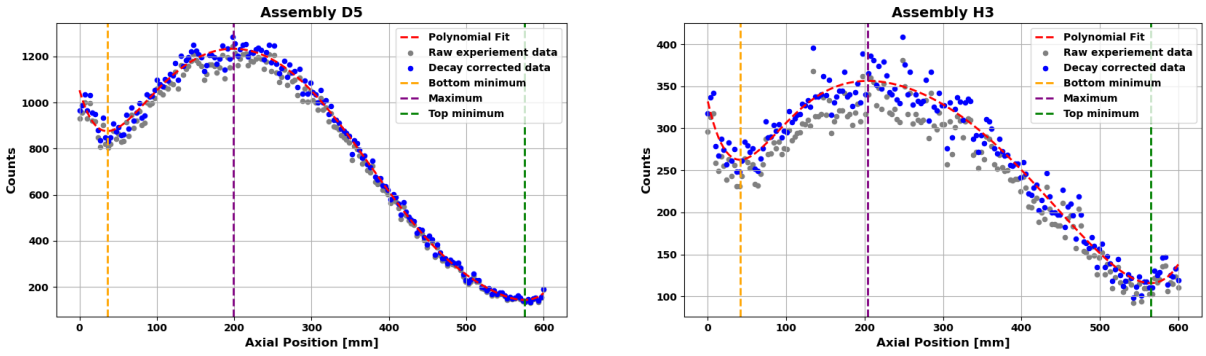

Figure 2: Experimental data, key features and decay corrected counts for assembly D5 (left) and H3 (right)

motivation of this study comes from the need to maintain accurate and reliable neutron flux measurements in the SAFARI-1 research reactor. The study's approaches are to (1) assess the stability of neutron flux key features and their relationship to the control bank positions, (2) detect anomalies of neutron flux measurements, and (3) validate the techniques used through statistical methods. To achieve these goals, the research uses polynomial fitting, statistical methods and likelihood function evaluation to obtain the errors of the key features. Hypothesis testing is

performed to evaluate trends of the observed changes and assess this in the context of the expected behavior.

2 Related Work

Statistical methods have been used to analyze and detect anomalies in the neutron flux profiles. For example, [5] employed a Bayesian statistical method found in Markov Chain Monte Carlo (MCMC) simulations to evaluate the neutron flux groups from activation data of different resulting isotopes at the Pavia University (Italy) TRIGA Mark II reactor. Their study showed promising results compared with Monte Carlo simulations of the reactor fluxes performed with the Monte Carlo N-Particle Transport (MCNP) code. Recent work has been done using statistical methods to detect anomalies in the neutron flux distribution. A recent study [6] used a combined method of anomaly detection and quantification for neutron flux data that considered delayed neutron monitoring data, significantly affecting reactor performance. Their proposed methods showed promising results and outperformed other anomaly detection methods regarding rates of false alarm, anomaly detection, and precision. Another recent study [1] focused on improving the accuracy of the neutron flux prediction in the SAFARI-1 research reactor using the statistical variance test and shift-correction procedure. The study used the t'Lam G statistical test to detect variance outliers and mean squared error (MSE) was minimized to correct flux shifts. The results demonstrated an improved magnitude and reduced the normalized root mean squared error (NRSME) for all the core positions, enhancing the accuracy of the flux prediction.

In this work, we proposed an approach to analyze key features of the neutron flux measurements (bottom minimum, maximum, and top minimum) and detect anomalies in the neutron flux profiles of the SAFARI-1 reactor. Specifically, use statistical metrics such as the standard deviation and mean absolute deviation (MAD) to assess the stability of the key feature points and their sensitivity to control bank positions using the Pearson's correlation coefficient, Spearman's rank correlation, Kendall tau correlation, and Xi correlation method.

3 Methodology

3.1 Decay Correction

In this study, to ensure accurate neutron flux measurements, a decay correction was applied to decay back the accumulated radioactive ^{64}Cu isotope during copper wire measurements. The activity of the ^{64}Cu isotope was corrected to the time at which the first data point of the first assembly was measured [7]:

$$\tilde{N} = Ne^{\lambda \Delta t}, \tag{1}$$

where N is the count measured at time t, $\tilde{N}$ is its decay-corrected value, $\lambda = 1.5160 \times 10^{-5}\ \mathrm{s}^{-1}$ is the decay constant for ^{64}Cu. In addition, the decay correction was applied for each of 180 data points along the wires to account for the radioactive decay during the measurement. Hence, for a point j of assembly i, the total time Δt was adjusted as follows:

$$\Delta t = (t_i - t_0) + j\delta t, \quad j = 1, \ldots, 180, \tag{2}$$

where j is the index of a measurement point along the wire, $\delta t = 1$ s represents the time taken to measure each data point, t_0 and t_i are the beginning of measurement times for the first assembly (wire) and assembly (wire) i, respectively.

3.2 Polynomial Fit

Decay-corrected neutron flux measurements from equation (1) were fitted using a polynomial of degree p, given that $F(x)$ are the neutron flux measurements,

$$P(x) = a_0 + a_1 x + a_2 x^2 + \ldots + a_p x^p, \tag{3}$$

where a_i are the polynomial coefficients generated by minimizing the squared error between $F(x)$ and $P(x)$. The first derivative of the polynomial $P'(x)$ was used to determine the extremes: bottom, maximum, and top minimum.

3.3 Variability Assessment

To assess the variability of key features found in (Eq. 3), the following equations are used:

$$\text{stdev} = \sqrt{\frac{1}{S}\sum_{s=1}^{S}(x_s - \bar{x})^2}, \quad \text{and} \quad \text{MAD} = \frac{1}{S}\sum_{s=1}^{S}|x_s - \bar{x}|, \tag{4}$$

where S represents the total number of key feature points, x_s represents the s-th key feature point at each cycle and $\bar{x}$ represents the mean of the key feature points [8].

3.4 Correlation Methods

The relationship between key features and control bank positions is calculated using equations in Table 1. The calculations of these correlation coefficients is to investigate which key feature is less sensitive to the movement of control rods.

Table 1: Correlation coefficients used in this study

Coefficient	Formula	Description
Pearson's r	$r = \frac{\sum_{i=1}^{n}(x_i - \bar{x})(y_i - \bar{y})}{\sqrt{\sum_{i=1}^{n}(x_i - \bar{x})^2 \sum_{i=1}^{n}(y_i - \bar{y})^2}}$	Measures the linear relationship between two variables [9].
Spearman's ρ	$\rho = 1 - \frac{6\sum_{i=1}^{n} d_i^2}{n(n^2-1)}$	Non-parametric test that measures the dependence between variables [9].
Kendall's τ	$\tau = 1 - \frac{\text{number of discordant pairs}}{\binom{n}{2}}$	Non-parametric test that measures the degree of association between variables [9].
Xi Correlation ξ	$\xi(X,Y) = 1 - \frac{n\sum_{i=1}^{n-1}\lvert r_{i+1} - r_i\rvert}{2\sum_{i=1}^{n} l_i(n - l_i)}$	Measure how much one variable is a function of the other [10].

3.5 Hypothesis Testing

To test whether the relationship between the three previously described key features and the bank positions is described by a linear function, the three key features, α, extracted from Eq. (3) and denoted as y_s^α, are fitted by the line $y^\alpha = m^\alpha x + c^\alpha$, at the bank positions x_s for cycle s and the errors σ_s^α. The key feature errors were evaluated by profiling the likelihood function of the data (using the MINOS algorithm of the Minuit package [11]). In this process, the data close to the extremum for each key feature was assumed to follow a quadratic shape (as the null hypothesis, H_0) and the likelihood function was taken as the Chi squared function. The errors for each bin of the flux profiles was scaled from its propagated Poisson value to achieve a reduced Chi squared value of one for this exercise. When evaluating the linear relationship for the three key features y_s^α as a function of bank position, the straight line was regarded as the null hypothesis and the likelihood function of the data was again taken as the Chi squared function. The errors σ_s^α had again to be scaled to achieve a reduced Chi squared value of one.

The critical chi-square value χ^2_{crit} is used to reject or accept the H_0 at a 95% confidence level:

$$\chi^2_{\text{crit}} = \chi_{1-\alpha,\text{dof}}, \tag{5}$$

with $\alpha = 0.05$, H_0 is rejected if $\chi^2 > \chi^2_{\text{crit}}$ and H_0 is accepted if $\chi^2 < \chi^2_{\text{crit}}$, dof is $N - \nu$ where N is the number of cycles and ν is the number of fit parameters.

4 Experiments & Results

The results of this study demonstrate a significant variation in neutron flux profiles within the SAFARI-1 research reactor, mainly due to control rod movement. Figure 3 shows the key features of the neutron flux profile measured at core position D5 (center of the reactor core). Table 2 provides the statistical information on these key features across cycles.

A high-order polynomial was successfully fitted to smooth the neutron flux measurements. This approach captures the distribution of these neutron flux measurements very well, enabling the calculation of key features shown by orange, purple, and green vertical lines in Figure 2.

The analysis focuses on three key features of the neutron flux profiles: bottom minimum, maximum, and top minimum. The results indicate that the maximum points have the highest variability compared to the other key features and are strongly positively correlated to control rod positions with Spearman's values of 0.5417 (including shifted measurements) and 0.5252 (excluding shifted measurements) for D5, 0.3582 (Including shifted measurements) and

0.3894 (excluding shifted measurements) for H3. In contrast, the bottom minimum showed lower variability and weaker correlations with Spearman's values of 0.3289 (including shifted measurements) and 0.3307 (excluding shifted measurements) for D5, 0.3331 (including shifted measurements) and 0.3560 (excluding shifted measurements) for H3. However, this key feature has missing values for some historical cycles, introducing a bias and inconsistencies in the analysis. The top minimum points demonstrated consistent results with standard deviation and MAD, and a moderate positive correlation with Spearman's values of 0.2432 (including shifted measurements) and 0.2358 (excluding shifted measurements) for D5, 0.3843 (including shifted measurements) and 0.4711 (excluding shifted measurements) for H3. The second part of this work was focused on estimating the errors

Table 2: Correlation analysis for D5 and H3

Position	Key Feature	Outliers	Std	MAD	Pearson	Spearman	Kendall	Xi
C-D5	Bottom Minimum	Including	9.32	7.52	0.282	0.329	0.222	0.069
		Excluding	9.06	7.51	0.291	0.331	0.224	0.120
	Maximum	Including	18.87	11.43	0.423	0.542	0.385	0.258
		Excluding	18.54	11.22	0.390	0.525	0.377	0.158
	Top Minimum	Including	16.72	7.47	0.201	0.243	0.167	0.080
		Excluding	9.64	6.70	0.196	0.236	0.163	0.049
C-H3	Bottom Minimum	Including	10.15	6.79	0.297	0.333	0.225	0.008
		Excluding	9.96	6.72	0.320	0.356	0.241	0.049
	Maximum	Including	21.91	13.46	0.331	0.358	0.238	0.116
		Excluding	22.43	14.18	0.350	0.389	0.256	0.131
	Top Minimum	Including	14.47	6.78	0.267	0.384	0.278	0.007
		Excluding	9.89	6.88	0.427	0.471	0.333	0.037

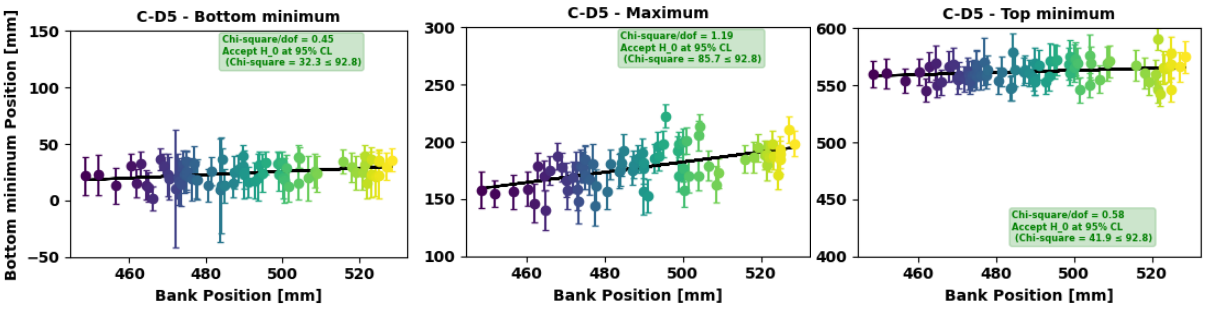

Figure 3: Bottom minimum, maximum, and top minimum along bank positions.

(uncertainties) of the key features, y_s^α, as described in the section on hypothesis testing. The error values of the neutron flux measurements were scaled by 1.5 to achieve a reduced chi square of ≈ 1. This indicates an additional systematic error source for the flux measurements. The profiled errors of the key features, σ_s^α, were then used in the linear trend hypothesis testing. Figure 3 indicates the linear trends and the chi-square values. Once again, the systematic errors, σ_s^α, had to be fractionally increased by 8 mm to attain a reduced chi-square of unity. The hypothesis testing is then applied on the Chi squared value described above. For the three key features, y_s^α, the linear hypothesis is accepted at the 95% confidence limit value. Additionally, the linear trends in Figure 3 have slopes of 0.145, 0.447, and 0.0931 for the bottom minimum, maximum, and top minimum key features, respectively.

Assembly H3 indicates higher variability and lower correlation, while D5 indicates low variability with high correlation. These findings are expected as H3 neutron flux measurements are noisier as they are located at the periphery and are distant from the control rods. In contrast, D5 is located in the middle of the reactor, where it experiences more of the effect of the control rods. The linear trend was accepted for all three cases. The slopes of the linear trends validated the different roles of the key features. Anomalies resulting from the incorrect insertion of copper

wires were detected by monitoring the positions of the top minimum points determined using a polynomial fit, as shown in Figure 2. These positions of the top minimum points allowed the detection of points that are outliers within the 500 mm to 600 mm range. Points deviating from the average within this range were identified as anomalies due to incorrect insertion of coppers wires. The study's findings provide insights into the relationship between key features and control rod movements and their reliability in estimating axially shifted neutron flux measurements.

5 Conclusion & Future Work

This study provides insight into the distributions of the neutron flux measurements in the SAFARI-1 research reactor, indicating the effect of control rod movement and copper wire insertions on neutron flux profiles. The research methodology involved data preprocessing, statistical analysis, and hypothesis testing. The study assessed the variability of key features and their sensitivity to control rod movement, indicating that the top minimum points of the neutron flux profiles are a stable and reliable means of estimating when these profiles are anomalous due to incorrect insertion of copper wires. Additionally, the anomalies due to incorrect insertion of copper wires were detected by tracking the positions of top minimum points, detecting outliers within the 500 mm to 600 mm range of the top minimum positions. These results demonstrated the importance of considering the features of neutron flux profiles when assessing reactor performance. Future research will include the development of data-driven techniques such as machine learning (ML) and artificial intelligence (AI) to detect axially shifted neutron flux measurements.

6 Acknowledgments

This study, as part of a master's project, is financially supported by Lesedi Nuclear Services. Lesedi Nuclear Services is hereby acknowledged with gratitude, and Necsa is acknowledged for the provision of additional neutron flux data.

References

[1] L. E. Moloko, P. M. Bokov, and K. N. Ivanov, "Estimation of the axial neutron flux profiles in the SAFARI-1 core using artificial neural networks," in *Proceedings of the International Conference on Mathematics and Computational Methods Applied to Nuclear Science and Engineering (M&C 2021), Virtual Meeting*, 2021, pp. 1644–1653.

[2] R. H. Prinsloo, O. Zamonsky, L. E. Moloko, B. Erasmus, and S. A. Groenewald, "SAFARI-1 benchmark description: IAEA CRP T12029," 2022.

[3] L. E. Moloko, P. M. Bokov, X. Wu, and K. N. Ivanov, "Quantification of neural networks uncertainties with applications to SAFARI-1 axial neutron flux profiles," in *Proceedings of the International Conference on Physics of Reactors (PHYSOR 2022), ANS, Pittsburgh, Pennsylvania, USA*, 2022, pp. 1398–1407.

[4] ——, "Prediction and uncertainty quantification of SAFARI-1 axial neutron flux profiles with neural networks," *Annals of Nuclear Energy*, vol. 188, p. 109813, 2023.

[5] D. Chiesa, E. Previtali, and M. Sisti, "Bayesian statistics applied to neutron activation data for reactor flux spectrum analysis," *Annals of Nuclear Energy*, vol. 70, pp. 157–168, 2014.

[6] D. Toshniwal, P. K. Gupta, V. Khurana, P. Upadhyay *et al.*, "Adq—anomaly detection and quantification from delayed neutron monitoring data of nuclear power plants," *IEEE Sensors Journal*, vol. 23, no. 7, pp. 7207–7216, 2023.

[7] M. Dawood, X. Jiang, and K. Schäfers, *Correction techniques in emission tomography*. CRC Press Boca Raton, 2012, vol. 69.

[8] S. Lee, "Comparing standard deviation and median absolute deviation (mad) metrics," https://www.numberanalytics.com/blog/comparing-standard-deviation-and-mad-metrics, 2025, retrieved July 18, 2025.

[9] M. Shaqiri, T. Iljazi, L. Kamberi, and R. Ramani-Halili, "Differences between the correlation coefficients pearson, kendall and spearman," *Journal of Natural Sciences and Mathematics of UT*, vol. 8, no. 15-16, pp. 392–397, 2023.

[10] S. Chatterjee, "A new coefficient of correlation," *Journal of the American Statistical Association*, vol. 116, no. 536, pp. 2009–2022, 2021.

[11] F. James and M. Roos, "Minuit," *CERN program library long writeup D*, vol. 506, p. 1993, 1994.